Restricting Involuntary Extension of Failures in Smart Grids using Social Network Metrics

Jose Cordova-Garcia[1,2], Dong-Liang Xie[1,3], Xin Wang[1]
[1] Department of Electrical and Computer Engineering, State University of New York at Stony Brook, USA
[2] Escuela Superior Politecnica del Litoral (ESPOL), Guayaquil, Ecuador
[2] Beijing University of Posts and Telecommunications, Beijing, China
jecordov@espol.edu.ec, xwang@ece.sunysb.edu, xiedl@bupt.edu.cn

***Abstract*—Modern communication technologies are expected to be available in the future Smart Grids to enable the control of equipments over the whole power grid. In this paper, we consider such networked control approach to address failures that may occur at any location of the grid, due to attacks or unit malfunction, and provide a wide-scale solution that prevent the failure impacts from spreading over a large area. Different from literature work that focuses on modifying power equations under the standard constraints of the power system, we estimate the impact of controlling different nodes on topological areas of the grid based on social metrics, which are derived from the graph capturing both the topological and electrical properties of the power grid. We propose a failure control algorithm for topological containment of failures in smart grid. Our algorithm also takes careful consideration of the impact the planned control has on the grid to avoid the possibly involuntary failure extension. We show that social metrics can efficiently trade off between the topological and electrical characteristics revealed by the power grid graph representation. We evaluate the performance against networked control strategies that only use power models to determine the actions to be performed at power nodes. Our results show that the proposed control scheme can effectively contain failures within their original location range.**

I. Introduction

The Smart Grid (SG) is envisioned to provide the necessary technology for a substantial improvement of monitoring and control applications of power systems. Failure control is arguably one of the most important applications. Failures can occur due to equipment malfunction, natural disasters, and planned attacks to grid infrastructure or systems. Legacy control and protection equipments often take automatic actions based on the local information. While such actions may address small-scale failures, the recent occurrence of large-scale failures has demonstrated the prevailing vulnerabilities of the grid and the need for the improvement of its control services [1], [2], [3], [4]. The amount of power flowing through a line plays a crucial role in the effectiveness of failure control as it is directly affected by failures and changes in the power grid. Following a failure or change, succeeding power flow redistribution can cause a power line to be tripped, and repeated failures would induce a cascading failure.

Different from substations and major equipments, it is unrealistic to assume that every power line in the grid is directly monitored and can provide reliable measurements. Due to the large number of power lines, instead of being equipped with a dedicated monitoring device, the majority of lines are monitored indirectly through other type of measurements such as voltage phasors. Also, many sections of the grid are either equipped with legacy monitoring devices that provide slow monitoring rates or even not observable at all.

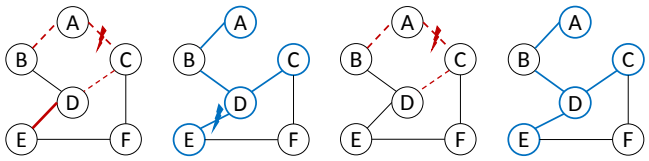

(a) Failure (b) Control (c) Failure (d) Control

Fig. 1: Failure control and its impact on the grid

In the examples of Figure 1, we illustrate two major problems, due to the unreliable monitoring and the use of conventional power control model respectively. The problem due to unreliable monitoring can be seen in Figure 1a. The power line (D, E), marked as the bold solid red line, is operating close to its thermal limit, beyond which the line will be disconnected and result in a failure. The Control Center (CC) is unaware of the critical status of (D, E), but meanwhile identifies a failure that occurs at (A, C). The failure effect on the power grid is marked with red dashed lines. A failure control policy is generated at the control center and transmitted to relevant power nodes using the communication network. Large changes caused by the failure control are marked as solid blue lines in Figure 1b. A failure control strategy that uses only power constraints has no restriction on the nodes to control and nodes/lines affected by the control. Suppose the control strategy following the basic power model has decided to change the loads of nodes A, D, C, E to address the failure, with the restrictions that all line flows do not exceed their capacity. While the failure at (A, C) has a distance from the critical line (D, E) and may not affect it greatly, the control action executed at nodes D, E does and a control due to inaccurate information may cause (D, E) to exceed its thermal limit. Hence, a new failure is induced, and *the original failure has been topologically extended.* Therefore, while the CC might have expected the communicated control actions to affect the region (lines) near the original fault, a topologically

978-1-5386-4128-6/18/$31.00 ©2018 IEEE

unrestricted policy may arbitrarily affect any region.

In Figure 1c, we can see another limitation of a control strategy solely based on power considerations. (D, E) now operates safely within its capacity limit and the impact of control shown in Figure 1d does not cause its disconnection. The coordinated control actions taken by all blue nodes are load shedding, and one may expect load reductions to affect the neighborhood of the region where the original failure is located. Although the control strategy may successfully address the failure, the locations of load shedding nodes are arbitrarily decided based on a power model without topological restrictions. As the load shedding reduces the amount of load that can be provided to the corresponding customers, from the customer view, the *effects of failure (i.e. the amount of demand yielded) are topologically extended.*

Both limitations discussed and illustrated above are the consequence of the lack of precise information and consideration of the topological impact a control strategy will impose on the grid. In this paper we address such limitations by using social metrics inferred from both the topological and electrical relationship of nodes in the power grid. While the graph concept is often applied to represent the physical topology of a network, there is little work to consider controlling the grid based on the graph from the electrical relationship perspective. Some recent studies have shown that social metrics can be used to characterize power grid vulnerabilities. Rather than just understanding the social relationship of grid nodes, we propose to leverage the observed social impact of power nodes on the grid to effectively control the grid failures while minimizing its indirect and involuntary effects on the grid status.

The rest of the paper is organized as follows. Section II reviews the related work on vulnerabilities of power grids and the control of failures. Section III describes the models used by our proposed algorithm. In Section IV, we analyze the social properties useful for the failure control, and describe the design of the control scheme proposed along with its algorithmic description. Section V describes the simulation scenario and the performance results. Finally, Section VI concludes the work.

II. Related Work

In recent years, power grid vulnerability analysis has drawn a lot of research attention. This analysis is necessary as a tool for designing more reliable power grids. Also, there is a substantial amount of work on applications and requirements that are feasible once modern communication systems become available in Smart Grids [5]. Timely planned failure control being arguably one of the most important applications.

Some recent studies represent the Smart Grid as a graph [6], [7] and study the properties of the electrical structure of the power grid. The goals are to identify "important" power nodes that can cause the biggest damage in case of failure (or attacks) through social metrics.

In [6] the authors propose to analyze an alternative graph representation of the power grid where links are constructed based on the strength of electrical connections in contrast to the physical power line connections. Instead of comparing the similarities between the topological and electrical graph structures, in this work, we study how nodes with different social properties impact the power grid *when controlled.* Moreover, different from [6], [7], our goal is to exploit the social properties of power nodes to determine the control strategy upon the occurrence of a failure.

Different from the traditional trigger-based automatic control and protection, the increasing adoption of modern communication technologies in power grids has provided the possibility of controlling failures in a planned, organized and coordinated way. Along the line of vulnerability analysis, the control strategies in [8], [9] attempt to maintain the power of the important nodes without shedding their load, where the important nodes are the ones that provide power to the control nodes. On the other hand, the recent work in [10] presents the methodology of identifying geographically correlated failures and evaluates the accuracy of its model using the historical data of the San Diego Blackout. The authors also present a standard control strategy based on the power model and its respective restrictions. In this paper, we agree on the general strategy of planned and coordinated control modeled by a mathematical program. However, different from the literature work, we make use of the graph representation of the power grid along with its topological and electrical properties to design the control strategy. Specifically, based on our observations of the graph's social properties, we provide the control program the capability of deciding control actions that prevent the topological extension of failures by reducing the effects of control-induced power flow redistribution on regions far away from the original failure.

III. Models

In this section, we present the system model used in the design of the control scheme. We start by introducing a commonly used graph representation of the smart grid and the components that are considered in the failure control process. Using this model, we describe how topological and electrical information can be inferred from the graph according to the model used for its edge weights.

A. Power Grid Model

A Smart Grid system contains two different networks: a power grid and a communication network to transmit data for the grid monitoring and control. The power grid will be modeled as a graph $\mathcal{P}(\mathcal{N}, \mathcal{E})$, where the $N = |\mathcal{N}|$ nodes include power generators, consumer loads and pass-through (transmission) substations. The physical power lines in charge of transmitting power from generation units to customer loads are contained in the edge set $\mathcal{E}$.

The communication network that provides monitoring and control capabilities can be modeled by a graph $\mathcal{P}'(\mathcal{N}', \mathcal{E}')$. If each node of the power grid is under the control, we will have an one-to-one mapping between the controllable nodes $\mathcal{N}'$ and the grid nodes $\mathcal{N}$. Although a communication network is often established along the power lines, the topology of the

communication network does not have to be exactly the same as that of the grid.

Each node $i \in \mathcal{N}$ in the grid $\mathcal{P}(\mathcal{N}, \mathcal{E})$ is associated with a power P_i, and is a power generator if $P_i > 0$ or a power consumer if $P_i < 0$. We consider a power grid to be balanced when $\sum_{i \in \mathcal{N}} P_i = 0$. The topology described by $\mathcal{E}$ captures the physical connections of power lines in the grid. Each power line $e_{i,j} \in \mathcal{E}$ has an operational capacity $c_{i,j}$, and its associated flow $f_{i,j}$ should be kept below $c_{i,j}$ for the normal operation. A line can be physically broken due to natural disaster or get disconnected by its protection equipment once it is overheated as a result of the sudden and frequent flow variation or because it works over capacity for an extended period of time. When there exist failures, we have $\sum_{i \in \mathcal{N}} P_i \neq 0$ and $\mathcal{P}(\mathcal{N}, \mathcal{E} \setminus \{e_{i,j}\})$, where the set of failed links are excluded from the power grid graph. Failures that cause long-term disconnections of lines can partition the grid into several components, in which case the models presented should be applied to each connected component.

B. Graph Weight Models

In the grid graph, the weight of an edge can correspond to the electric parameters (i.e. admittance) associated to it or the physical distance of the power line corridor that links two nodes (substations). We use the topological distance to reflect the geographical distance, and $d_{i,j}$ to represent the shortest distance between a pair of nodes i and j. Power flows can also be used as weights $w(e_{i,j}) = f_{i,j}, \forall e_{i,j} \in \mathcal{E}$ and a failure location would be identified by the edge whose flow exceeds the capacity threshold. However, power lines can operate over the capacity for some time before being tripped. For more effective and timely failure control, it is more informative to identify the locations where flows are changing. A power flow model is often applied to describe the behaviors that govern the power grid and how flows change and traverse the nodes and edges in $\mathcal{P}$, but it does not directly reflect the topology information. However, the admittance matrix used in flow models can be interpreted as a weighted Laplacian of the grid graph $\mathcal{P}$, and the admittances of the lines can be used as weights for the graph to capture both the graph relationship and power interaction. Specifically, the elements of the admittance matrix $\mathbf{Y}$ are defined as:

$$Y_{i,j} = \begin{cases} \sum_{k \neq i} y_{i,k} & \text{if } i = j \\ -y_{j,i} & \text{if } i \neq j, \end{cases} \tag{1}$$

where $y_{i,j} \in \mathbb{C}$ is the line admittance and it only exists if the physical connection between i and j exists. Different from the literature work which uses the admittance matrix to identify vulnerable components or only refers to the admittance matrix when describing the power flow models [11], [8], [9], [10], we will exploit graph-based metrics that can infer topological and electrical information from $\mathbf{Y}$ to contain failures in power grids to prevent their propagations to a large area.

IV. Topological Containment of Failures in Smart Grids

The aim of this work is to control grid failures while minimizing the indirect and involuntary detrimental effects on the grid caused by the control. We first introduce the issues involved when performing the optimal load shedding to control the grid failures. We then discuss two types of centrality metrics adapted from social networks to the power grid network, and examine the effect of using social power nodes on controlling failures over a typical grid topology. Finally, based on the insight gained from our observations, we describe the design of an optimal control scheme based on social metrics.

A. Load Shedding-based Failure Control

A power grid operating out of its normal state, e.g. due to power imbalance and/or power-line overcapacity, can return to its normal state by adjusting the total power in the network. Load shedding actions can help restore the power balance and make the power flows to be under their capacity limits. A basic mathematical formulation of such a control involves the optimization of a function of the controllable loads, $P_i \in \mathbf{P}$, in a way that the reduction from the power amount at the time of failure, P_i^0, is minimized, subject to a tractable power flow model and the capacity constraints:

$$\begin{aligned} \underset{P_i \in loads}{\text{minimize}} \quad & \mathbf{1} \cdot (\mathbf{P} - \mathbf{P}^0) && \text{(2a)} \\ \text{subject to} \quad & \mathbf{P} = \mathbf{Y} \cdot \mathbf{\Theta}\,, && \text{(2b)} \\ & f_{i,j} = \beta \hat{f}_{i,j} + (1-\beta) f_{i,j}^0\,, && \text{(2c)} \\ & f_{i,j} \leq c_{i,j}\,,\ i,j \in \mathcal{N} \mid e_{i,j} \in \mathcal{E}\,, && \text{(2d)} \\ & P_i^0 \leq P_i \leq 0, \forall i \in loads && \text{(2e)} \\ & 0 \leq P_i \leq P_i^0, \forall i \in generators && \text{(2f)} \end{aligned}$$

The constraints (2b) and (2d) represent the power model with the voltage vector $\mathbf{\Theta}$ and the capacity limits for the power lines, while (2e) and (2f) represent the load and generation limits. Each active power P_i in (2b) correspond to $\sum_{j \in N(i)} f_{ij} = P_i, \forall i, j \in \mathcal{N}, (i,j) \in \mathcal{E}$ and $N(i)$ is the set of neighbors of i. Equation (2c) estimates the evolution of the power flow $f_{i,j}$ after control, where β is a tuning parameter [10], $\hat{f_{i,j}}$ is the theoretical power flow calculated using (2b), and $f_{i,j}^0$ is the flow of the power line $e_{i,j}$ at the moment of failure. Thus, the model of the operating condition of a line, $f_{i,j}$, in (2c) incorporates the thermal effect of changing the flow $f_{i,j}^0$. The performance of this model depends on the timely and reliable transmission of the value $f_{i,j}^0$ from its monitoring device.

Simply reducing the total amount of load may require nodes all around the grid to change loads, so customers at locations distant from the original failures may be also affected. Also, as discussed in Section I, altering the load of a node can cause power flow changes in lines relatively far away from the node. In case that a critical line is affected, this will introduce more uncertainty in control effectiveness. Moreover,

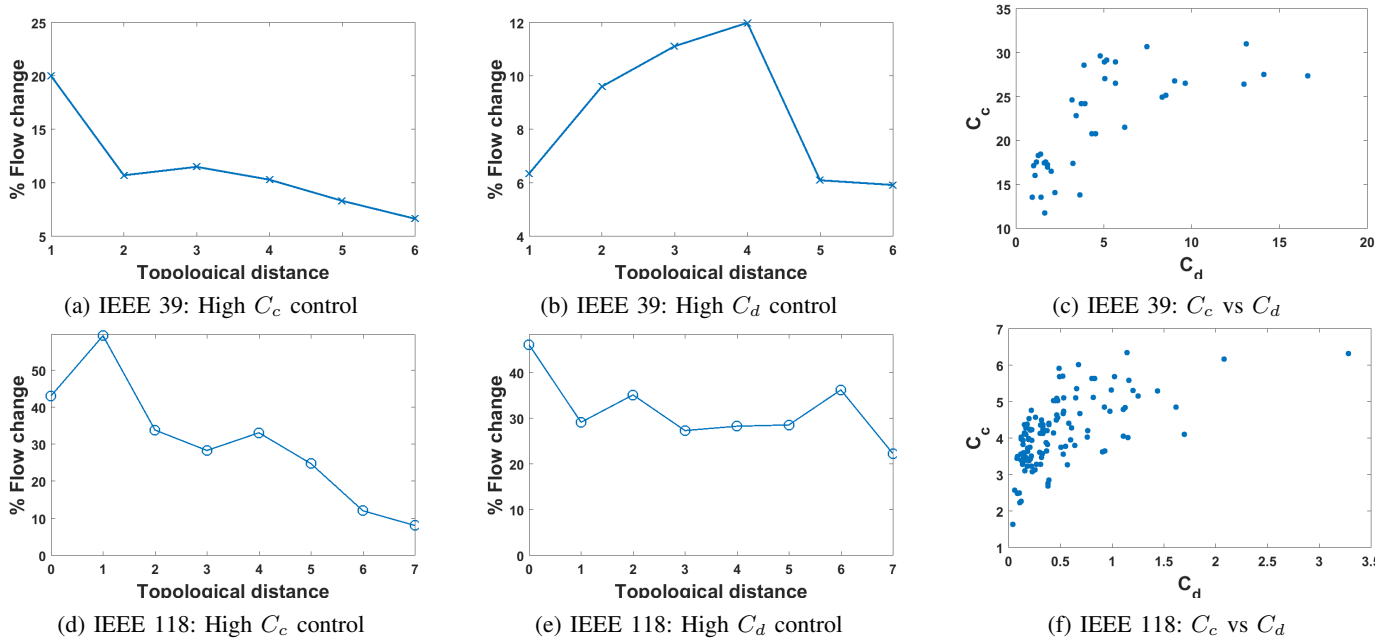

(a) IEEE 39: High C_c control (b) IEEE 39: High C_d control (c) IEEE 39: C_c vs C_d

(d) IEEE 118: High C_c control (e) IEEE 118: High C_d control (f) IEEE 118: C_c vs C_d

Fig. 2: Using centrality to select controlled nodes: Average flow changes at different distances from the location of the control node.

controlling loads all over the grid is more prone to loss and delay of control packets, which can take the network to unplanned states, temporarily or permanently. The variability of flows at the unplanned states contribute to the overheating of the power lines and/or the false tripping which further extends the failure. Furthermore, while the power variables involved in (2) are related with the graph representation of the grid, no characteristics or information that can be extracted from the graph is used in this control formulation. A control strategy as the one described before could assign the amount of load shed as a function of the distance in an effort to geographically contain the failure expansion and the impact of control. However, different from communication networks or social networks where mainly the network graph is considered, power grids are governed by physical characteristics that have to be taken into account when defining their topology and constraining the control extension. Next, we describe the physical features of the grid that can be adapted from its graph representation to design the control scheme.

B. Topological/Electrical features of the Grid

In order to constrain the failure extension to a large geographic distance, we also need to consider the tradeoff between physical topology connections and the inherent electrical coupling that governs the distribution of flows and consequently defines the status of the grid and its stability. The admittance matrix $\mathbf{Y}$ can be used to describe the electrical coupling of nodes and lines in the grid.

An "electrical" connection represented by $r_{i,j}$ can be defined along with the physical connection $e_{i,j}$ described in $\mathcal{P}(\mathcal{N}, \mathcal{E})$ to measure the impact on the grid after modifying the power of a controlled node. Analogous to the length (distance) of a power line between two nodes $e_{i,j}$, the electric *resistance* distance is defined as [12]:

$$r_{i,j} = z_{i,i} + z_{j,j} - 2z_{i,j} \tag{3}$$

where $z_{i,j} \in \mathbf{Z} = \mathbf{Y}^{-1}$. The electric resistance distances in $\mathbf{R}$ describe the connectivity between any pair of nodes i, j. Thus a matrix $\mathbf{R}$ can be defined to capture all resistance distances in the grid. As the power grid is known to have a sparse topology, the matrix $\mathbf{Y}$ is sparse because its entry $y_{i,j}$ corresponds to the admittance of the power line $e_{i,j}$ which physically connects i and j. Hence, its inverse $\mathbf{Z}$ is a full matrix with entries $z_{i,j}$ even for the case $e_{i,j} \notin \mathcal{E}$.

To contain a failure and its effects, we need to consider both the topological and electrical closeness between the controlled nodes and the failure location. As the physical topology information is embedded in $\mathbf{Y}$ and the electric coupling is described with the matrix $\mathbf{R}$, our control criteria will incorporate both factors. In light of the metric from social network, we consider building up from two centrality metrics to capture the impact of the control of a specific node on the overall grid nodes: *closeness centrality* and *degree centrality*.

Different from studies that asses the impact of social-node failures/removals on the grid to identify system vulnerabilities, we focus on investigating the impact of controlling central nodes to define a control scheme that leverage social characteristics to restrict the failure extension.

C. Closeness Centrality and its Impact on Control

In order to evaluate the impact of power flow change of a node on other nodes, we would like to have a metric *electric closeness centrality* to determine how "close" a controllable

node is to all other nodes. This may be evaluated in terms of the electric resistance distance as:

$$C_c(i) = \frac{1}{\sum_{j=1}^{N} \frac{r_{i,j}}{N-1}}, \tag{4}$$

where $r_{i,j}$ of the matrix $\mathbf{R}$ contains the electric distance between nodes i and j in the network, and $\mathbf{R}$ is a full matrix. Analogous to the social network closeness centrality, when a node i with a high electric closeness centrality performs a change (control), it is expected to have a great impact on the grid.

However, unlike a social network, power networks are also subject to a power model to determine how flows traverse the nodes. To verify this, we perform a preliminary study to evaluate the closeness centrality metric of the IEEE 39 and IEEE 118 bus systems [13]. We select the top 10 nodes with higher closeness centrality to evaluate the percentage of the flow change they impose on the grid when load shedding is performed at these nodes. For illustration purpose, the amount of load shedding is randomly selected within a range of 5% to 20%, so the flow changes correspond to the average change induced by different levels of load shedding.

In Figures 2a and 2d, the flow change is measured for all power lines represented by the topological edge $e_{k,l} \in \mathcal{E}, k, l \in \mathcal{N}$, and we show the average flow change as a function of the topological distance from the controlled nodes.

By the analogy to the social metrics, nodes with the high closeness centrality are expected to have a great influence on the network. However, in Figure 2a and 2d, we can see that large changes in the grid states such as power flows are contained within a distance. This implies that controlling a high $C_c(i)$ node allows us to reduce the amount of flow directed to it while restraining the rest of the flow changes. This can be explained by the fact that in the power grid, the closeness centrality of a node i describes how likely it is for the power to flow to or through the node. However, while large changes are contained within a distance, the flow changes may not exhibit the desired decreasing trend as seen in the largest peak of figure 2d.

Thus, the electrical closeness reveals some important features of nodes in the power grid, and some of these features can be carefully exploited to control these nodes to topologically contain the failures with a decreasing effect with distance.

D. Degree Centrality and its Impact on Control

Besides the closeness centrality, to capture the coupling of a power node with the rest of the components of the grid (power lines and nodes), we will investigate another measurement of centrality, *electric degree centrality*:

$$C_d(i) = \frac{|| Y_{i,i} ||}{N-1}, \tag{5}$$

where $Y_{i,i}$ is the corresponding entry of the diagonal component of $\mathbf{Y}$, the admittance matrix. This measurement of centrality considers the total admittance of power lines terminating at the node i. Different from $C_c(i)$, it captures the physical connections instead of *all* the electrical connections.

Similar to the analyses with the closeness centrality, we select the top 10 nodes ranked with the highest degree centrality, $C_d(i)$. In Figures 2b and 2e, compared to the control of nodes with high closeness degree, large effects of controlling nodes with high degree centrality appear to expand to longer topological distances from the controlled location. Thus, while C_d alone may not provide a favorable impact on the grid, the degree centrality of a node can provide information about the large peaks that interrupt the decreasing trend of flow changes from the controlled point. Hence, $C_d(i)$ will be used in our design with $C_c(i)$ to quantify the effect of controlling the node i for the failure recovery.

E. Failure Control based on Social Metrics

Our preliminary observations have shown that social centrality metrics can be applied to more effectively control the failure in the power grid. We showed that the closeness and degree centralities contain different information that can be leveraged for control. However, some nodes may have high values for both types of centralities as shown in Figures 2c and 2f. The two metrics can be used to trade off between controlling nodes topologically close to the failure and controlling nodes whose electric impact is low but may be distant from the failure. The latter can prevent impacting power lines from uncertain monitoring, at the cost of controlling nodes possibly far from the original failure location. Next, we need to determine the amount of load to shed at a controllable node to contain failures.

The metric $C_c(i)$ helps identify how electrically close a node i is to the rest of the network and quantify the impact of load change at i on the overall grid. On the other hand, the metric $C_d(i)$ helps identify nodes that have a high coupling with the grid based on the physical connections and characteristics of power lines. Thus, the amount of load shed at a controllable node i should be a function of three factors: its possible impact on the grid, its physical connections, and its electrical characteristics.

Following our previous observations, the desired decreasing trend of flow changes is sometimes interrupted by large peaks when controlling nodes with C_c alone. Then, $C_d(i)$ can be used to address the limitation of C_c as it provides information of the effect at longer topological distances. Therefore, we consider the ratio $\frac{1}{C_d(i)C_c(i)}$ as a proportion factor of the amount of load to shed. This factor considers both the impact at locations close and the impact at longer topological distances as described by the social metrics. In this centrality factor, the contained impact described by $C_c(i)$ is dominant as it can be seen from (5) that the variance of $C_d(i)$ is much less than that of $C_c(i)$. In this way, we use $C_d(i)$ as a weight for $C_c(i)$ that will constrain shedding to not be abrupt and contribute to a smoother decreasing trend.

Moreover, failures can occur anywhere in the network, and it is desirable to constrain the impact on loads to nodes close to

the failure locations. Controlling nodes based solely on their centrality factor can restrict the impact of load changes to nodes near the controlled node, but these changes may not be restricted to be close to the failed node if a node with small $\frac{1}{C_d(i)C_c(i)}$ rank is far from the failure location. We will further consider the impact due to both the electric and topology distances from the controllable node i to the failure. For a single-line failure located at $e_{j,k}$, we can define an electrical-topological distance to each controllable node as:

$$\bar{r}_{i,e_{j,k}} = \left(1 - \frac{r_{i,e_{j,k}}}{\sum_{i\in\mathcal{N}} r_{i,e_{j,k}}}\right) d_{i,e_{j,k}} \tag{6}$$

where, $d_{i,e_{j,k}}$ is the topological distance from node i to line $e_{j,k}$ which can be defined analogously to the electrical distance to an edge. Then each node $i \in \mathcal{N}$ can use the aforementioned metrics to determine the amount of load to be shed by defining:

$$\alpha(i) = \frac{1}{C_d(i)C_c(i)} \frac{\bar{r}_{i,e_{j,k}}}{\sum_{i\in\mathcal{N}} \bar{r}_{i,e_{j,k}}} \tag{7}$$

In (7), we model a mixed metric of social centralities and topological/electrical distances. The centrality factor provides the information of i's impact when controlled. A node with a large $\frac{1}{C_d(i)C_c(i)}$ is more likely to impact largely the grid and should have less load shedding when controlled. The normalized factor $\bar{r}$ helps balance the topological and electrical distances to the failure location. The metric in (7) can be used to provide a weighted version of equation (2), which determines the amount of load shedding at each node.

Finally, to further minimize the direct effect of load shedding on the power delivered to customers, a regularization term can be added to the objective function of Eq. (2). With the regularization term, the sparsity of the solution of the control problem can be controlled. In this way, the regularization term contributes to the minimization of the number of (large) control actions required to address a failure. Moreover, as the proposed scheme corresponds to networked control, it is desirable to have fewer control message transmissions, in order to reduce the chance of delaying or missing control packets thus the possible compromise of the reliability of the control scheme. The objective in Eq. (2) can be modified as:

$$\boldsymbol{\alpha} \cdot (\mathbf{P} - \mathbf{P}^0) + \lambda \mid\mid \mathbf{P} - \mathbf{P}^0 \mid\mid \tag{8}$$

where λ is the regularization parameter that induces the control algorithm to require large shedding to the least number of nodes as possible. Thus, the number of nodes that can have great impact is reduced. Algorithm 1 summarizes the proposed control approach. Step 7 details that the control algorithm will optimize (8) which in turn makes controlled nodes perform power changes proportionally to αs. When there are multi-line failures, we can apply the proposed control by adapting (6) and (7) to use the topological-electrical distance from the controllable node i to the closest failed line $e_{j,k} \in F_0$, where F_0 is the set of failed lines. Furthermore, calculating the different metrics involved in (7) requires the matrix $\mathbf{Y}$, its (pseudo)-inverse and simple arithmetical computations, which are known a priori by the control center and can be calculated offline. After identifying failures, the control center can update $\mathbf{Y}, \mathbf{Z}$. For very large networks, as well as common real life implementations, a distributed version of Algorithm 1 can be implemented to improve the scalability of the control, where the proposed metric (7) does not increase the complexity of such a task.

Algorithm 1 Social Based Control

INPUT: Power Grid graph $\mathcal{P}(\mathcal{N}, \mathcal{E})$, set of initial line failures $F_0 \subset \mathcal{E}$

1: Calculate $\mathbf{R}$
2: **for all** $e_{j,k} \in F_0$ **do**
3: Obtain candidate nodes $N_{e_{j,k}} \subset N$
4: **for all** $i \in N_{e_{j,k}}$ **do**
5: Compute load shedding contributions $\alpha(i) \in \boldsymbol{\alpha}$: $\alpha(i) = \frac{1}{C_d(i)C_c(i)} \frac{\bar{r}_{i,e_{j,k}}}{\sum_{i\in N_h} \bar{r}_{i,e_{j,k}}}$
6: **end for**
7: Compute eq. (2) with objective: $\boldsymbol{\alpha} \cdot (\mathbf{P} - \mathbf{P}^0) + \lambda \mid\mid \mathbf{P} - \mathbf{P}^0 \mid\mid$, using $\alpha(i)$ to determine the load sheddings.
8: **end for**
9: Transmit control actions to all nodes $i \in N_{e_{j,k}}, \forall e_{j,k} \in F_0$

V. Performance Evaluation

In this section, we evaluate the performance of the proposed control scheme and its capability of restraining failures and their effects when restoring the power grid status back to its normal operation. Here, the topological extension of a failure is measured by the effect that control actions have on power flow changes in all the lines of the grid.

We compare the performance of the proposed control (Algorithm 1) with a topologically unrestricted load shedding control strategy proposed in [10], based on (2) and refer to it as *standard control*. Standard control only makes use of the power flow equations that govern the behavior of the power grid, and the restrictions imposed on its equipments e.g. power flow capacities.

A. Simulation Scenario

We evaluate two different scenarios, which are differentiated by the location of the failure that triggers the control process: targeted attacks and random failures. In the targeted attack scenario, there is a disconnection of a node with high centrality. That is, there is an attack against the power lines of the targeted node. As discussed in Section IV-D, C_d is a local metric directly related to the number of lines associated to node i. Thus, it is more likely that an attacker could estimate such centrality nodes without requiring complete information of the power grid. Hence, the metric used to select the failure location (faulted node) is the degree centrality as defined in (5). We also evaluate the scenario where the failure of a power node occurs at a random location in the power grid.

The test cases used for evaluation correspond to IEEE bus systems of different sizes. Such cases are based on portions of

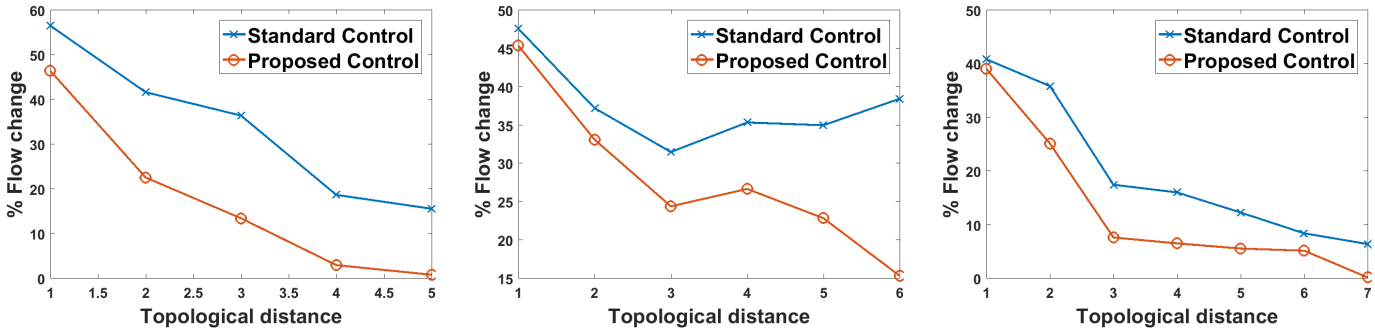

(a) IEEE 39 (b) IEEE 57 (c) IEEE 118

Fig. 3: Targeted Failures: Average flow changes due to failure control at different distances from the location of failure.

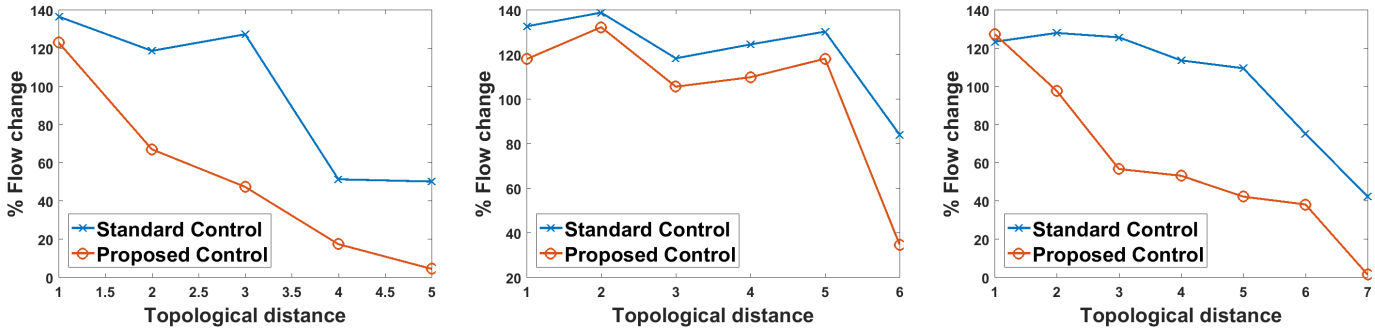

(a) IEEE 39 (b) IEEE 57 (c) IEEE 118

Fig. 4: Targeted Failures: Maximum flow changes due to failure control at different distances from the location of failure.

the American Electric Power System, e.g. New England IEEE 39 bus system. Besides having a variety of sizes, different IEEE test cases also present different topologies, which in turn impact the social metrics. Thus, the 39, 57, and 118 test cases allow us to evaluate the scalability of the proposed solution.

B. Impact of Control on Power flows

The execution of a failure control strategy causes an amount of flow change in all power lines of the grid. Figure 3 shows the average amount of power flow change, due to control, at different distances from the original failure location.

The x-axis indicates the topological distance (in number of hops) from the power line to the failure location. The goal of our control strategy is to restrain such great changes to occur in locations as close as possible to the original failure locations and provide a monotonically decreasing trend for such changes.

When a failure occurs at a high centrality node, the proposed scheme properly assigns different levels of load shedding in a way that the shedding on power flows decreases with the distance from the failure location. Figure 3 shows a clear monotonically decreasing trend of power flow changes with distance. Moreover, such a trend is present regardless of the power grid evaluated, which demonstrates the scalability of our solution.

On the other hand, the standard control is driven only by the power flow equations, and thus can perform relatively large control (shedding) away from the failure. Thus, the standard control can include more nodes that are of higher centrality rather than the ones close to the failure. Furthermore, without restriction on the controlled nodes, the standard control can choose to perform load shedding at high centrality nodes without considering the effect of such actions on the grid.

As discussed before, controlling high degree centrality nodes can have a relatively large effect on the grid even at locations far away from the controlled node. Such effect results in the occurrence of peaks of flow change at power lines far away from the failure location as shown in Figure 3b, where the decreasing trend achieved by the proposed control is slightly interrupted at the hop 4 with a small peak. This is a consequence of controlling nodes that have high values for both types of centralities. In this case, the centrality factor in (7) will result in large shedding for such nodes and farther away flows are impacted as with the standard control. Fortunately, the distance factor in Equation (7) takes effect to properly restrain peaks at far away nodes to be as small as possible. Figure 4 helps to visualize such effects, where the maximum flow change recorded for the targeted failures scenario is presented. Note the maximum flow change of a line does not imply that the line exceeds its capacity, but only indicates how much change it experiences in order to control the failure while working within its line capacity limit. The figure shows that the peaks of flow change can reach

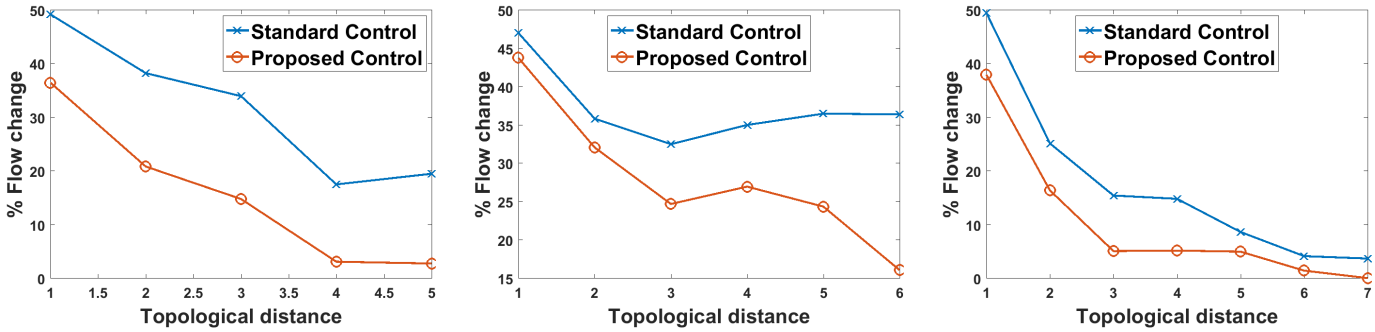

(a) IEEE 39 (b) IEEE 57 (c) IEEE 118

Fig. 5: Random Failures: Average flow changes.

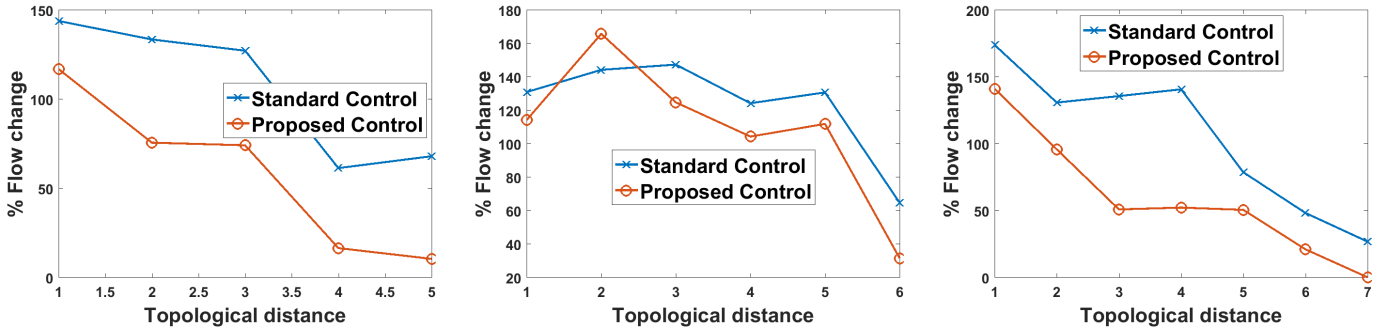

(a) IEEE 39 (b) IEEE 57 (c) IEEE 118

Fig. 6: Random Failures: Maximum flow changes.

considerably large values. For example, Figures 3c and 4c reveal that while on average both control schemes show similar monotonic behavior, there exist cases where the flow change caused by the standard control can be more than double that by the control based on the social metrics. Similarly, in Figure 4b, our proposed control shows a few considerable large peaks of flow changes that resemble those of the standard control. However, Figure 3b shows that on average the control based on social metrics can restrict the propagation of effects several times smaller than that from the standard control. Moreover, using the recorded maximum flow change, a power operator can track and identify the node whose disconnection results in this behavior and provide preventive measures to address the vulnerability of such particular grid.

Figures 5 and 6 show results when the failure location is randomly selected without considering the centrality of the affected node. It can be inferred that failures that involve high centrality nodes dominate the performance of control, as our control scheme again effectively applies the electrical-topological distance along with the centrality information metric to capture the possible effect of controlling every node in the grid when taking shedding actions. Thus, the similarity of the trends in both scenarios suggests that social metrics can be used to identify the nodes that would cause the most damage to the grid, as also reported in related power grid vulnerability studies.

As discussed in Section I, restraining the propagation of control effects close to the original failure location is extremely important in case power lines are unknowingly operating near their capacity limit. The standard control relies on the assumption that the capacity constraint accurately describes the line status and the monitoring of the status of all power lines in the grid is timely and reliable. In contrast, we have seen that our social scheme, without relying on the monitoring information, provides a "decaying with distance" control effect that will become benefitial in presence of critical lines.

C. Impact of Measurement Reliability

Now we evaluate the effect of monitoring conditions on the efficiency of a failure control strategy. In the previous evaluations, we have considered that all edges are working within their capacity limits at the moment of failure, and their states are timely known when the control strategy is calculated. Now we randomly select 10% of the grid edges to be operating at full capacity, where a power flow increase will cause the line to be tripped. At the same time, we generate failures that trigger the control process, and evaluate the 3 locations of interest as done before.

In the following evaluations we vary the reliability to describe the amount of information the control center has about the sensitive edges. The impact of the reliability on the control efficiency is presented in terms of the system yield, i.e. the ratio of total demand supplied at the stable state after

the failure to the total demand supplied before the failure. The yield is affected proportionally to the amount of load shedding decided by the control strategy. In the case of 100% reliability, a control strategy should be able to stop the failure and take the network back to the stability. In the case of 0% reliability, none of the sensitive lines could inform its condition to the control center. However there exist some power lines that are affected significantly while being far away from the failure, which compromises its performance. When the reliability decreases, a control strategy may not be able to bring the grid back to the stability due to new failures. Then, a new control strategy needs to be communicated to the grid until it reaches the stability. We show these results in Figure 7.

If part of the states of the sensitive lines are known, the standard control can prevent only this portion from failure. As its strategy is not restricted by locations, its impact can still affect the sensitive lines not reliably monitored. On the other hand, the proposed control topologically restricts failures and controls its impact along with the information from part of the sensitive lines, and can obtain about 30% more yield than the standard control for the monitoring unreliability cases. This can be seen in the case that failures are randomly located across the grid in Figure 7b.

When failures occur near high C_c nodes, it is more likely for control actions to be performed close to the failure locations. However, the standard control can still affect varied locations across the grid away from failures. Then, when the reliability decreases, the performance of the standard control is significantly compromised due to the lack of consideration of the topological extent of its control actions. In Figure 7a, we can see that our control maintains its smooth increasing trend, providing almost 28% more yield than the standard control when the reliability decreases.

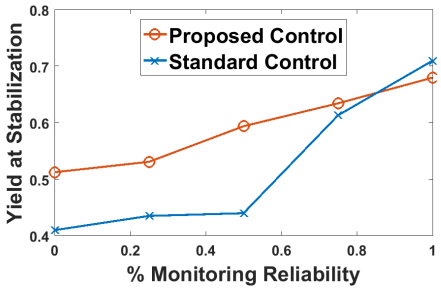

(a) Targeted Failures.

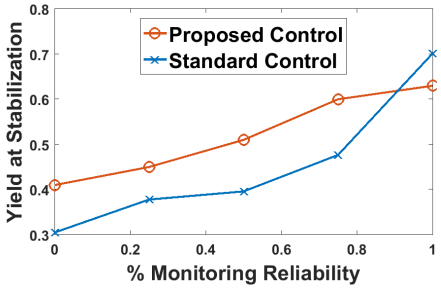

(b) Random Failure.

Fig. 7: Effect of power flow monitoring reliability on Yield.

VI. Conclusion

The load control of grid nodes without considering the topological information may result in the involuntary disconnection of power lines unknowingly operating at their capacity limits, which leads to the extension of power grid failures. We show that social metrics derived from the graph representation of the grid can be used to infer the impact of failure control and the possible topological extension of the problem. We propose a networked control scheme based on the social metrics along with a metric that balances the topological and electrical closeness of controllable nodes. Compared to the conventional schemes, our performance results demonstrate that control based on social metrics can effectively restrain the failure and the impact of control to be close to the original failure locations. Moreover, even when the states of sensitive power lines are unknown, the impact of the proposed control on those lines is still considerably reduced.

References

[1] U.S.-Canada Power System Outage Task Force. Final report on the august 14, 2003 blackout in the united states and canada: Causes and recommendations, April 2004.

[2] UCTE. Final report of the investigation committee on the 28 september 2003 blackout in italy. 2004.

[3] Xiangyi Chen, Changhong Deng, Yunping Chen, and Chunyan Li. Blackout prevention: Anatomy of the blackout in europe. In *Power Engineering Conference, 2007. IPEC 2007. International*, pages 928–932, Dec 2007.

[4] Chunyan Li, Yuanzhang Sun, and Xiangyi Chen. Analysis of the blackout in europe on november 4, 2006. In *Power Engineering Conference, 2007. IPEC 2007. International*, pages 939–944, Dec 2007.

[5] V.C. Gungor, D. Sahin, T. Kocak, S. Ergut, C. Buccella, C. Cecati, and G.P. Hancke. A survey on smart grid potential applications and communication requirements. *Industrial Informatics, IEEE Transactions on*, 9(1):28–42, 2013.

[6] E. Cotilla-Sanchez, P.D.H. Hines, C. Barrows, and S. Blumsack. Comparing the topological and electrical structure of the north american electric power infrastructure. *Systems Journal, IEEE*, 6(4):616–626, Dec 2012.

[7] Zhifang Wang, A. Scaglione, and R.J. Thomas. Electrical centrality measures for electric power grid vulnerability analysis. In *Decision and Control (CDC), 2010 49th IEEE Conference on*, pages 5792–5797, Dec 2010.

[8] M. Parandehgheibi, E. Modiano, and D. Hay. Mitigating cascading failures in interdependent power grids and communication networks. In *SmartGridComm Communications and Networks Symposium. IEEE*, November 2014.

[9] M. Rahnamay-Naeini and M.M. Hayat. On the role of power-grid and communication-system interdependencies on cascading failures. In *Global Conference on Signal and Information Processing (GlobalSIP), 2013 IEEE*, pages 527–530, Dec 2013.

[10] A. Bernstein, D. Bienstock, D. Hay, M. Uzunoglu, and G. Zussman. Power grid vulnerability to geographically correlated failures; analysis and control implications. In *INFOCOM, 2014 Proceedings IEEE*, pages 2634–2642, April 2014.

[11] L. Galbusera, G. Theodoridis, and G. Giannopoulos. Intelligent energy systems: Introducing power-ict interdependency in modeling and control design. *Industrial Electronics, IEEE Transactions on*, 62(4):2468–2477, April 2015.

[12] D.J. Klein and M. Randi. Resistance distance. *Journal of Mathematical Chemistry*, 12(1):81–95, 1993.

[13] University of Washington. Power systems test case archive.